

BULLETIN OF THE CHEMICAL SOCIETY OF JAPAN, VOL. 45, 1299—1305(1972)

Ionization Energies and Rydberg States of Tetraaminoethylenes

Yoshihiro NAKATO, Masaru OZAKI,* and Hiroshi TSUBOMURA

Department of Chemistry, Faculty of Engineering Science, Osaka University, Toyonaka, Osaka

(Received September 13, 1971)

Absorption spectra and photo-ionization curves of tetrakis (dimethylamino) ethylene, (TMAE), and 1,1',3,3'-tetramethyl- $\Delta^{2,2'}$ -bi(imidazolidine), (TMBI), have been studied. It has been found that these compounds have very low ionization potentials (about 5.4 eV), which are even comparable with that of the lithium atom. The first ionization potentials of these compounds are nearly the same, although both their absorption spectra and their photo-ionization curves are considerably different from each other. These results can be explained semi-quantitatively by use of the results of simple, semi-empirical molecular orbital calculation with inclusion of direct interaction between four lone-pair orbitals on the N atoms, which was found to be important at the "perpendicular" structure. The first absorption bands of these molecules are assigned to the Rydberg bands, lying quite unusually near the visible region. The quantum defect δ is found to be 0.7 for the lowest Rydberg state of TMAE. The size of the Rydberg orbital for this state is estimated to be 2.9 Å from the maximum radial density, which is comparable with the core size. Higher Rydberg series are also observed for TMBI.

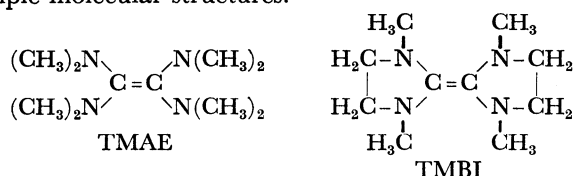
Ionization potentials of organic compounds are one of the key quantities in the studies of electronic processes in organic materials, such as organic semi-conductors, organic photo-conductors, and formation and reactions of electron-donor-acceptor complexes. The gas-phase ionization potentials of organic compounds

reported so far lie in the range of about 7 to 12 eV.¹⁾ Recently, we have found that tetrakis (dimethylamino)-ethylene, (TMAE), and 1,1',3,3'-tetramethyl- $\Delta^{2,2'}$ -bi(imidazolidine), (TMBI), have extremely low ionization

1) K. Watanabe, T. Nakayama, and J. Mottle, *J. Quant. Spectry. Radiative Transfer*, **2**, 369 (1962); F. I. Vilesov, *Usp. Fiz. Nauk. (SSSR)*, **81**, 669 (1963). English Translation, *Soviet Phys. USPEKHI*, **6**, 888 (1964).

* Present address: Asahi Chemical Industry Co., Ltd. Tokyo.

potentials, about 5.4 eV, in spite of their relatively simple molecular structures.²⁾



The fact that dialkylamino groups have strong electron donating properties is well known. Tetraaminoethylenes have as many such groups as possible for a substituted ethylene, and hence are very strong electron-donors. The chemical properties of these interesting compounds have been studied extensively and they are characterized as electron-rich olefins³⁾ or as strong electron donors.⁴⁾

The knowledge on the electronic structures of tetraaminoethylenes is, however, still rather limited. The electron donor strength, the bonding and the electronic spectra for TMAE were interpreted by a simple HMO calculation.⁴⁾ The electronic spectra were also explained qualitatively in terms of intramolecular charge transfer mechanism.⁵⁾

There have been some difficulties, both experimental and theoretical, in the study of the electronic structure of the tetraaminoethylenes. In the first place, they are strongly reactive to oxygen, emitting strong luminescences. The experiments with them must, therefore, be made with extreme care. Secondly, there is some ambiguity as to their molecular conformations. It is expected that a large steric repulsion exists between four dialkylamino groups. This may prevent the tetraaminoethylenes from taking the "planar" structures and make their conformations more or less uncertain. The "non-planar" structure may lead to a breakdown of the π -electron approximation. Namely, the lone-pair orbitals on the N atoms overlap not only with the π -orbitals on the C atoms, but also directly with the other lone-pair orbitals, and with the σ -orbitals. Finally, the role of the molecular Rydberg states in the low-lying excited levels has been overlooked.

In the present paper, the results of measurements on the photo-ionization curves, ionization potentials and absorption spectra will be reported, together with the discussions on the electronic structures and ionization potentials of free molecules in the gas phase, based on the MO calculations of these molecules.

Experimental

Both TMAE and TMBI were prepared according to the literature.⁶⁾ Crude products were distilled in an atmosphere

2) Y. Nakato, M. Ozaki, A. Egawa, and H. Tsubomura, *Chem. Phys. Lett.*, **9**, 615 (1971).

3) R. W. Hoffmann, *Angew. Chem.*, **80**, 823 (1968); *Angew. Chem. Internat. Edit.*, **7**, 754 (1968).

4) N. Wiberg, *Angew. Chem.*, **80**, 809 (1968); *Angew. Chem. Internat. Edit.*, **7**, 766 (1968).

5) M. Hori, K. Kimura, and H. Tsubomura, *Spectrochim. Acta*, **24A**, 1397 (1968).

6) For TMAE, R. L. Pruett, J. T. Barr, K. E. Rapp, C. T. Bahner, J. D. Gibson, and R. H. Lafferty, Jr., *J. Amer. Chem. Soc.*, **72**, 3646 (1950). For TMBI, H. E. Winberg, U. S. 3239518, 3239519 (1966).

of nitrogen under reduced pressure. They were then degassed and distilled repeatedly in a vacuum line, and stored in evacuated glass ampoules with breakable seals. *n*-Pentane, isopentane, and methylcyclohexane were passed through silica gel columns, left overnight in contact with sodium wire and distilled. All the sample solutions were prepared by dissolving TMAE or TMBI through breakable seals into solvents after they had been completely deoxygenated. Absorption spectra of TMAE and TMBI at room temperature were measured by using various cells with path length ranging from 1.0 to 10 cm.

Absorption spectra in the wavelength region longer than 190 nm were measured in a Cary Model 15 spectrophotometer. Both absorption spectra and photo-ionization curves in the wavelength region between 300 and 155 nm were measured by a 0.5 meter Nalumi vacuum monochromator. It has a Bausch and Lomb concave grating (concave radius 498.1 mm, ruled area 30 mm \times 51 mm, 600 grooves/mm, blazed at 1500 Å, blaze angle 2°35'). The plate factor of the monochromator is calculated to be 28.3 Å/mm when the grating is used in the first order at $\lambda=150$ nm. The slit width used was normally 200 μ . The light source used is a hot-cathode-type hydrogen-discharge lamp from Mitsubishi Electric Corp., operated at 0.9 A and 70 V, which emits photons of the wavelengths longer than 155 nm. A Toshiba 7696 photomultiplier (S-11 type) covered with a sodium salicylate thin film is used as a photon detector. Emission lines from mercury and hydrogen lamps were used to calibrate the wavelength scale. The stray light was found to be less than 3% of the total light from the exit slit around 160 and 180 nm.

Photon absorption and photocurrent were measured as functions of photon energy in the same run. A pyrex cell used has two quartz windows (transparent down to 155 nm) and two collecting-electrodes held parallel to each other by means of tungsten wire-pyrex seals, the resistance between which was 3×10^{15} ohms at 25°C. Photocurrent was measured by Takeda Riken vibrating reed electrometer, TR-84M. The applied voltage between electrodes was 5 to 10 V in normal use. In the above experimental conditions, the minimum photocurrent detected was about 2.0×10^{-15} A. Estimating the light intensity at some 10^9 photons/sec from the photomultiplier output, the photo-ionization yield ($=\sigma_i/\sigma$) can be measured to be at least 2×10^{-5} , if it is assumed roughly that one half the incident light was absorbed by the sample vapor (where σ and σ_i are absorption and photo-ionization cross sections, respectively).

Results

Absorption spectrum of TMAE in the vapor phase is shown in Fig. 1. At least four transitions may be involved in the spectrum which are centered at 29.0, 38.5, 44.8, and 53.0 kK. The first (29.0 kK) and the second (38.5 kK) bands agree closely with those reported by Winberg, Downing, and Coffman,⁷⁾ and the fourth (53.0 kK) agrees with that by Hori, Kimura, and Tsubomura.⁵⁾ Some structures are seen in the region around the fourth band. Near ultraviolet absorption spectra of TMAE in MP solutions, both at room temperature and 77°K, are given in Fig. 2 together with that in the gas phase, where MP is a mixed solvent consisting of methylcyclohexane and isopentane in a volume ratio of 1:1. Similar spectrum was ob-

7) H. E. Winberg, D. R. Downing, and D. D. Coffman, *J. Amer. Chem. Soc.*, **87**, 2054 (1965).

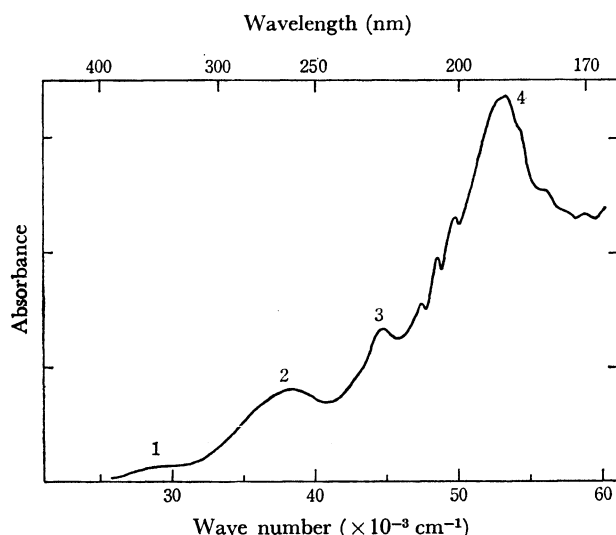


Fig. 1. The absorption spectrum of TMAE in the vapor.

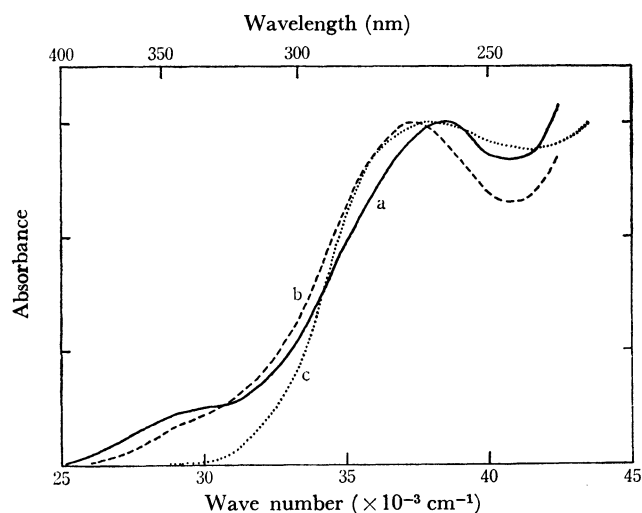


Fig. 2. The absorption spectra of TMAE in the near UV region; curve a (—) for the vapor, curve b (---) for an MP solution at room temperature and curve c (.....) for the same solution at 77°K. The profile around the second band (38 kK) of curve c is somewhat ambiguous, because the matrix became a little opaque.

tained in an *n*-pentane solution or in an ether solution, and a maximum was found at 45.5 kK. The absorption maxima previously reported are 37.3 kK in *n*-heptane, tetrahydrofuran and acetonitrile,⁵⁾ and 37.0 and 45.2 kK in *n*-decane.⁸⁾ The agreements are good.

Absorption spectra of TMBI both in the vapor and in an *n*-pentane solution are shown in Fig. 3. Vapor absorption begins at about 25.0 kK and increases towards higher wave numbers with a few inflexions (32.8 not clear, 35.7, 40.8 kK). The first peak is located at 50.5 kK. The second seems to exist at around 60 kK or higher.

It should be noted here that the first band of TMAE shifts to higher wave numbers in an MP solution at room temperature compared with that in the vapor although the second band shifts rather inversely. The first band is apparently missing at 77°K. The

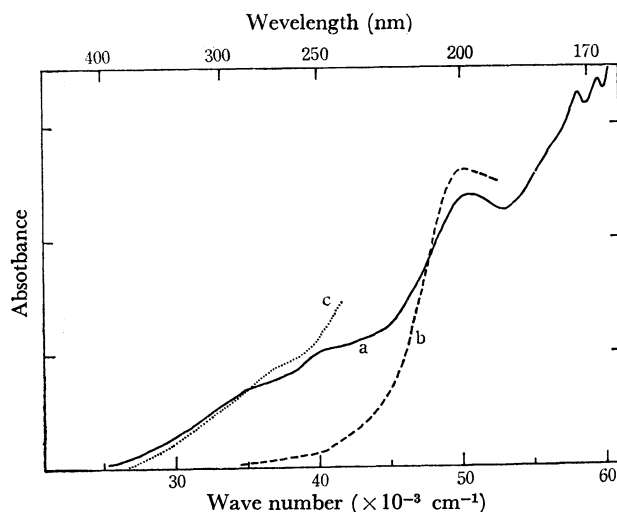


Fig. 3. The absorption spectra of TMBI; curve a (—) for the vapor, curve b (---) for an *n*-pentane solution at a low concentration of TMBI and curve c (.....) for the same one at a high concentration.

absorption spectrum at wave numbers lower than 45 kK for TMBI in the vapor is also apparently missing in an *n*-pentane solution.

Very recently, several studies concerning the Rydberg states in condensed media were made.^{9,10)} The main conclusion is that the Rydberg band is sensitive to the environments surrounding the molecule. It moves to shorter wavelengths when it is placed in the condensed phase or even in the gaseous state at high pressure.¹¹⁾ The first band of TMAE and the bands in the near UV of TMBI show behaviors similar to the Rydberg bands reported in these papers, so that it may be concluded that they are Rydberg bands. It may also be concluded that the second and third bands of TMAE and the 50.5 kK band of TMBI are non-Rydberg bands from their insensitiveness to the environments. The fourth band of TMAE also seems to be non-Rydberg, because it is too strong to be assigned to the Rydberg band. This conclusion is supported by the molecular orbital calculation.

It must be pointed out here that the gas-phase absorption spectrum of TMAE seems to contain an underlying continuous absorption which increases in intensity towards higher wave numbers, as seen in Fig. 1. This may be concluded to correspond to the transitions to the higher Rydberg series and the ionization-continuum. A similar feature is seen for the gas-phase spectrum of TMBI in Fig. 3.

Figure 4 shows the photo-ionization curves for TMAE. Curve a shows the relative photo-ionization cross section, σ_i^{rel} , as a function of photon energy, E , and curve b is the first derivative curve ($d\sigma_i^{\text{rel}}/dE$ vs. E). σ_i^{rel} was calculated at every 10 Å by using the equation, $\sigma_i = \sigma \cdot i / (I_0 - I)$, where σ , i , and $I_0 - I$ are the relative absorption cross section, photocurrent and relative light

9) B. Katz and J. Jortner, *Chem. Phys. Lett.*, **2**, 437 (1968), and the papers cited therein.

10) A. J. Merer and R. S. Mulliken, *Chem. Rev.*, **69**, 639 (1969).

11) M.B. Robin and N.A. Kuebler, *J. Mol. Spectrosc.*, **33**, 274 (1970).

8) C. A. Heller and A. N. Flechter, *J. Phys. Chem.*, **69**, 3313 (1965).

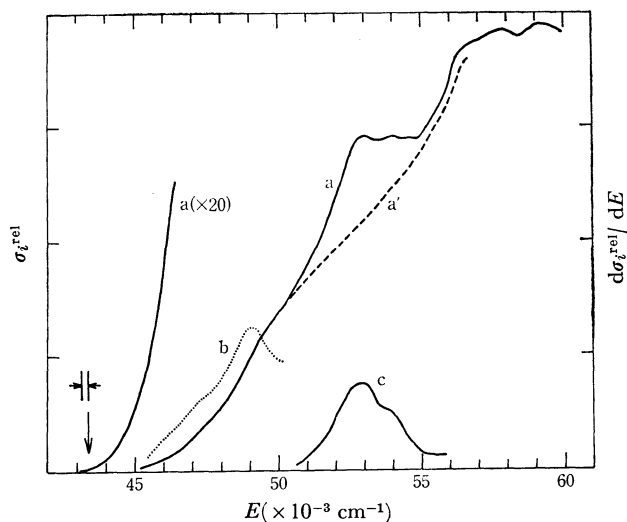


Fig. 4. Gas-phase photo-ionization of TMAE; curve a shows σ_i^{rel} vs E and curve b $d\sigma_i^{\text{rel}}/dE$ vs. E . Curve a is divided into curve a' and c in the energy region around 53 kK, which are estimated to correspond to the contributions of the direct ionization and the auto-ionization, respectively. (See text.). The threshold for photo-ionization is shown by an arrow. The energy spread of the photon beam at the threshold is also indicated.

intensity absorbed by the sample vapor, respectively. The onset of the ionization is rather gradual. Such a feature is common to those reported for aliphatic and aromatic amino compounds.^{12,13)} In such cases, it is difficult to determine the adiabatic ionization potentials accurately. We have, therefore, taken the point of appearance of σ_i^{rel} as an upper limit for the first adiabatic ionization potential.

Curve a has three steepest slopes at 49, 52, and 56 kK, and curve b has maxima at these positions, as shown only for the first steepest slope in Fig. 4. According to Morrison's method,¹²⁾ the first vertical ionization potential for TMAE can be determined to be 49.3 kK from the maximum of curve b. The second

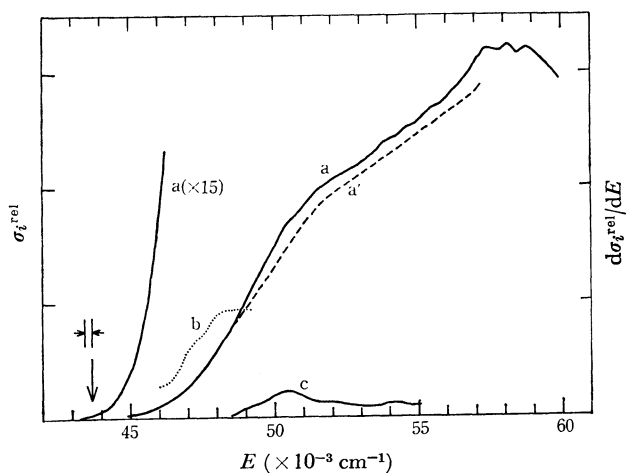


Fig. 5. Gas-phase photo-ionization of TMBI. Each curve and mark are indicated in the similar manner as in Fig. 4.

12) H. Hurler, M. G. Inghram, and J. D. Morrison, *J. Chem. Phys.*, **28**, 76 (1958).

13) M. Batley and L. E. Lyons, *Mol. Crystals*, **3**, 357 (1968).

steepest slope at 52 kK, however, seems to be attributable to the auto-ionization from the fourth band of TMAE, rather than to the second (direct) ionization. The estimated curve for the direct ionization is shown as curve a' (a broken line) and the difference between the curves a and a' is shown as curve c, which corresponds to the contribution due to the auto-ionization. This interpretation may be supported by the fact that curve c agrees very well with the fourth band in Fig. 1. If this is the case, the second vertical ionization potential may be estimated to lie in 55–56 kK.

Photo-ionization curves for TMBI are shown in Fig. 5, from which the ionization potentials can be determined in the same way. The auto-ionization also seems to occur, but is not so clear. The first vertical ionization potential estimated to lie around 49 kK is, therefore, made somewhat uncertain. The second photo-ionization seems to start at about 57 kK.

Photo-ionization curves in the higher wave number regions (≥ 57 –58 kK), both in Figs. 4 and 5, seem to be less reliable, because of the line spectrum of the hydrogen lamp used as the light source.

The observed ionization potentials are summarized in Table 1, together with those reported in the literature.

TABLE 1. GAS-PHASE IONIZATION POTENTIALS

		the first I_p		the second $I_p^{(e)}$
		adiabatic	vertical	vertical
TMAE	this work	≤ 5.36	6.11	ca. 6.9
	literature a)	< 6.5		
	literature b)		6.27	
TMBI	this work	≤ 5.41	~ 6.1	ca. 7.1

a) From the appearance potential of the parent ion in the mass spectrum; N. Wiberg and J.W. Buchler, unpublished.

b) Calculated from the difference in the charge-transfer absorption maxima for TMAE and dimethylaniline as the donors and nitrobenzene as the common acceptor, where 7.35 eV for the ionization potential of dimethylaniline was used; Ref. 15). This should be compared with the vertical value obtained by us.

c) These are only tentatively estimated values.

MO Calculations

In order to understand the experimental results, it seems worthwhile to make theoretical calculations of the electronic energies. For the purpose to find the orbital energies of filled π -MO's and to characterize the π - π^* type transitions, a simple semi-empirical molecular orbital calculation was made using only the $2p\pi$ -AO's on the C atoms and the lone-pair AO's on the N atoms. Each of the lone-pair AO's is assumed to be one of the sp^3 hybrid orbitals of the nitrogen atom. The details of the method of calculation is given in the Appendix.

The molecular conformations of tetraaminoethylenes have not been fully established. The planar $N_2C=CN_2$ skeleton can at least be assumed for the ground state. The inspection of the molecular model shows that the

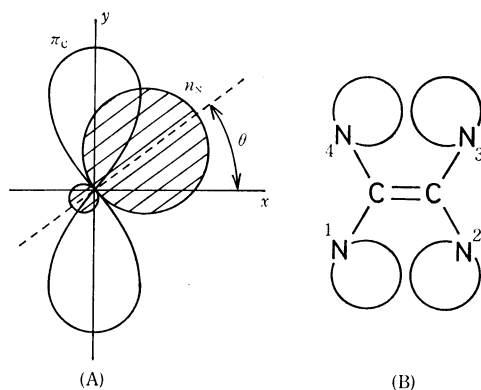


Fig. 6. (A), A projection of a nitrogen lone-pair AO and a carbon $2p\pi$ -AO on the xy plane perpendicular to the C-N bond. The angle θ is indicated. (B), The "perpendicular" structure of tetraaminoethylenes. Only the $N_2C=CN_2$ skeleton and four lone-pair orbitals are illustrated.

four dimethylamino groups have some freedom of twisting around each of the four C-N bonds. Let the direction of a C-N bond be the z -axis, and we draw the projectories of carbon $2p\pi$ -AO and nitrogen lone-pair AO on the xy plane as shown in Fig. 6 (A). Then, the angle θ as shown in Fig. 6 (A) can be the best parameter to define the conformation of the dimethylamino group. The C-N resonance interaction (β_{CN} in the Appendix) makes the "planar" structure ($\theta=90^\circ$ in Fig. 6 (A)) the most preferable, which is, however, more or less prevented by the mutual steric repulsion between the crowded methyl groups. The infrared absorption spectrum of TMAE shows no band in the $\nu_{C=C}$ regions,¹⁴ whereas an intense $\nu_{C=C}$ band (1630 cm^{-1}) appears in the Raman spectra.⁷ TMAE also gives only one sharp proton signal in the NMR spectrum.^{7,14} All these results suggest that the molecular conformation is symmetric with respect to the C=C bond. At present, the most reasonable model for TMAE in the ground state seems to be a "perpendicular" structure ($\theta=0^\circ$) under wobbly motion proposed by Hammond and Knipe,¹⁵ in which the $(CH_3)_2N$ groups are vibrating about a position "perpendicular" to the $N_2C=CN_2$ plane. TMBI gives two sharp proton signals in the NMR spectrum. The steric repulsion between the methyl groups for TMBI seems to be much less than that for TMAE, but may still be large enough to prevent the complete "planar" structure.

The complexity of the problem arises from the fact that each of the four dimethylamino groups has a certain free domain of wobbly motion, and there are quite a number of possible conformations for TMAE. For TMBI, the situation is somewhat similar, although there is a geometrical restriction of cyclization for the twisting motions. In order to describe various conformations, we start from the "perpendicular" structure, in which all lone-pair orbitals lie on the $N_2C=CN_2$ plane in the manner as shown in Fig. 6 (B), and construct all other conformations by twisting dialkylamino groups about the C-N bonds with angles of θ_i , where

14) N. Wiberg and J. W. Buchler, *Z. Naturforsch.*, **19b**, 5 (1964).

15) P. R. Hammond and R. H. Knipe, *J. Amer. Chem. Soc.* **89**, 6063 (1967).

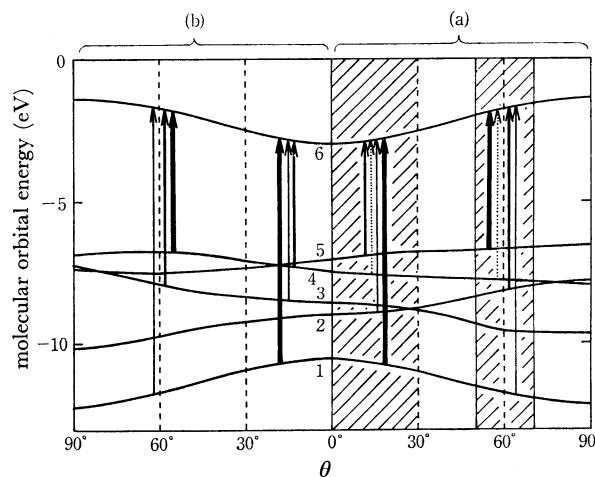


Fig. 7. Molecular orbital energies for tetraaminoethylenes. Each molecular orbital energy is plotted as a function of θ , for two types of conformations, (a) and (b). The Slater's parameter (μ) used is 1.80.

i ($i=1,2,3,4$) is numbering of dialkylamino groups as shown in Fig. 6 (B). The angle θ_i is defined so as to have a positive value on twisting the lone-pair orbital upwards.

The calculation has been made for various possible conformations, *i.e.*, at various θ_i values each independent of others. Part of the results obtained is shown in Fig. 7. Here, the molecular orbital energies are plotted as a function of θ for two types of conformations: (a), $\theta_1=\theta_3=-\theta_2=-\theta_4$ ($=\theta$) and (b), $\theta_1=\theta_4=-\theta_2=-\theta_3$ ($=\theta$). Each of these two types of conformations, especially (a), is expected to have the least steric repulsion between the methyl groups. The orbital energies of the four lone-pair orbitals are split by the direct N-N interaction into those of four MO's at the "perpendicular" structure ($\theta=0^\circ$). As the angle θ increases, this N-N interaction decreases, while the interaction between N and π_C becomes important. Consequently, somewhat complicated curves with several cross-points are obtained, as seen in Fig. 7.

Of the six MO's, which are numbered at $\theta=0^\circ$ as shown in Fig. 7, the lower five are filled with electrons, and only the highest is vacant. Allowed transitions under the approximation described in the Appendix¹⁶ are indicated by arrows in Fig. 7; those having strong transition moments by thick arrows and those having weak transition moments by thin arrows. Arrows with dotted lines indicate those with negligibly small transition probabilities. The transition probabilities are found to depend strongly on θ . From the consideration of steric hindrances, it is assumed that the allowable region of θ for TMAE is from 0° to 30° and that for

16) The transition moments calculated for the conformation (a) under the approximation described in the Appendix are as follows, $\mu(6\leftarrow 5)^2$: $\mu(6\leftarrow 4)^2$: $\mu(6\leftarrow 2)^2$: $\mu(6\leftarrow 1)^2=0.00$: 0.00 : 0.00 : 1.00 at $\theta=0^\circ$; 0.69 : 0.00 : 0.29 : 0.54 at $\theta=30^\circ$; 1.29 : 0.02 : 0.54 : 0.17 at $\theta=60^\circ$; 1.45 : 0.04 : 0.56 : 0.08 at $\theta=90^\circ$, where $\mu(n\leftarrow m)^2$ indicates the square of the transition moment from the m -th MO to the n -th MO in Fig. 7 relatively. The transition, $6\leftarrow 3$, is symmetry forbidden for the conformation (a). The transition moments change continuously with θ . Similar results are obtained for the conformation (b).

TMBI from 50° to 70°, which are marked by hatching for the conformation (a) in Fig. 7.

The results obtained are summarized as follows.

(1) The energy of the highest filled MO is nearly the same in the two regions; $\theta=0^\circ$ —30° and 50°—70°, as seen from Fig. 7. (Inversion of the highest filled MO's occurs for the conformation (b)). This result agrees with the observation that TMAE and TMBI have almost equal ionization potentials. The low ionization potentials of these molecules compared with the alkylamine and ethylene seem to be caused mainly by the direct N—N interaction for TMAE and mainly by the C—N resonance interaction for TMBI.¹⁷⁾

(2) We have concluded in the previous section that the first band of TMAE (Fig. 1) is of Rydberg nature. From the results of calculation made for the conformation (a) in the region $0^\circ \leq \theta \leq 30^\circ$, it is shown that the 6←1 transition indicated in Fig. 7 is mainly of the nature of π - π^* transition in the ethylenic group and is therefore very strong. The transitions, 6←5 and 6←2, are shown to be forbidden at $\theta=0^\circ$ but become considerably strong near $\theta=30^\circ$.¹⁶⁾ The theoretical predictions for the relative intensities of these three transitions agree fairly well with those observed for the second, third, and fourth bands in the TMAE absorption spectrum, though they are made somewhat ambiguous owing to the presence of the underlying continuum, as mentioned in the preceding section. The transition, 6←4, is predicted to be negligibly weak, and is probably hidden by other strong bands. Similar good agreements are also found for the conformation (b) in the region $0^\circ \leq \theta \leq 30^\circ$.

(3) In the region $50^\circ \leq \theta \leq 70^\circ$, the transition energies are much larger than the corresponding transition energies at $\theta=0^\circ$ —30° both for the conformations (a) and (b). This explains very nicely the marked blue-shift of absorption bands observed for TMBI compared with those for TMAE, since it has been concluded in the previous section that the 50.5 kK band of TMBI corresponds to the lowest allowed valence transition (6←5 in Fig. 7(a) or 6←4 in Fig. 7(b)).

We have assumed that TMAE and TMBI take the structure represented by either the conformation (a) or the conformation (b). These two conformations are expected to be preferred owing to their least steric repulsions between methyl groups. It might be possible, however, that TMAE and TMBI take structures represented by mixtures of these two and other conformations with the less steric repulsions between the methyl groups. Even in such cases, the above-mentioned conclusion is not substantially altered.

Discussions

The above mentioned calculated and observed results seem to provide fairly convincing explanation as to the question why TMAE and TMBI have nearly the same

ionization potentials (I_p 's), although they are expected to have different conformations.

Although the first vertical I_p 's of TMAE and TMBI are easy to determine from the $\sigma_{\text{ion}}^{\text{cal}}$ curves, only the upper limits are obtained for the adiabatic I_p 's. It seems, however, very likely from the following consideration that these observed limits lie close to the true adiabatic I_p 's. The nuclear configuration of TMAE in the Rydberg state is expected to be similar to that of the positive ion, as pointed out for ethylene.¹¹⁾ Therefore, the difference between the adiabatic and vertical energies for the Rydberg transition will be nearly equal to that for the ionization. The difference between the vertical and adiabatic energies for the first Rydberg transition of TMAE is estimated fairly accurately to be about 0.6 eV, because the adiabatic energy for this transition can be obtained from the overlapping part of the absorption and fluorescence spectra. The difference between the observed limit for the adiabatic I_p and the vertical I_p determined in the present work for TMAE is about 0.7 eV as seen from Table 1, which is in fairly good agreement with the difference between vertical and adiabatic energies of the first Rydberg transition.

The large differences between the vertical and adiabatic I_p 's for both TMAE and TMBI should be attributable to large change of the molecular conformations upon ionization. It is suggested that TMAE⁺ has nearly "planar" structure from the ESR studies.^{4,18)} It must also be pointed out that a large difference (~0.7 eV) was reported even for aliphatic amines,¹³⁾ possibly because of the change of the molecular shapes from the pyramidal structures to the planar.

We have assigned the first band of TMAE and a number of low-lying bands of TMBI to the Rydberg bands on the basis of their characteristic behaviors in solutions compared with those in the vapor. The higher series for TMAE may be covered by the stronger second band corresponding to the transition to the valence state. These unusually low-lying Rydberg states for tetraaminoethylenes are naturally expected from their very low I_p 's.

The term values of Rydberg states in molecules fall into a series, expressed in the form,

$$T = RZ^2/(n^*)^2 = RZ^2/(n-\delta)^2,$$

where, Z is the charge on the core, R the Rydberg constant, n^* the effective principal quantum number. From this equation, and using the adiabatic I_p and the wavelength at the center of the overlap between the first absorption band and the fluorescence spectrum, n^* is calculated to be 2.3. If this band is assumed to be the first member of the series ($n=3$), δ then becomes 0.7. The empirical δ -values reported for the Rydberg series of molecules built-up from atoms of the first period are 0.9—1.2 for ns -series, 0.3—0.5 for np -series and 0.1 for nd -series.¹⁹⁾ Deviation of the quantum defect, δ , for the first Rydberg state of TMAE from

17) Strictly speaking, the interaction with the σ -electrons must be included, especially at small θ . It is, however, expected from a simple consideration that this interaction causes little change for the highest filled MO in Fig. 7. R. Hoffmann, A. Imamura, and W. J. Hehre, *J. Amer. Chem. Soc.*, **90**, 1499 (1968).

18) K. Kuwata and D. H. Geske, *ibid.*, **86**, 2101 (1964).

19) G. Herzberg, "Molecular Spectra and Molecular Structure III. Electronic Spectra and Electronic Structure of Polyatomic Molecules," D. Van Nostrand Co., Inc., Princeton, N. J., (1966). p. 341.

either those for ns or np -series, as seen above, may be attributable to the large departure of the core potential from spherical symmetry. The size of the Rydberg MO can be roughly estimated from the equation, $r_0 = (n - \delta)^2 a_0 / Z$, where a_0 is 0.529 Å and r_0 is the r -value at which the radial density has its maximum. We obtain $r_0 = 2.9$ Å for the first Rydberg state of TMAE. On the other hand, it is thought that the positive charge of the core is located mainly on the four equivalent N atoms, since the highest filled MO consists mainly of the four lone-pair orbitals on the N atoms. The size of the core is, therefore, comparable with r_0 obtained above, since the N-N distances of TMAE are about 2.7 and 2.4 Å.

A large Stokes' shift between the first absorption and fluorescence bands is observed for TMAE. This large Stokes' shift was attributed by some authors to the conformational change of the fluorescent state of TMAE from the ground state, in the former of which the two N_2C halves are assumed to be perpendicular to each other in the $N_2C=CN_2$ skeleton.^{4,9} This explanation seems to assume that the first band is due to a π - π^* type transition. As discussed in the foregoing of this section, however, it seems more likely that the fluorescent state takes a structure similar to $TMAE^+$, in which the planarity of the skeleton is maintained.

Appendix

A simple LCAO MO theory is used in this work. Normalized symmetry orbitals, ξ_i , are first constructed as follows,

$$\begin{aligned}\xi_1 &= (2 + 2S_{CC})^{-1/2}(\chi_{Ca} + \chi_{Cb}) \\ \xi_2 &= (2 - 2S_{CC})^{-1/2}(\chi_{Ca} - \chi_{Cb}) \\ \xi_3 &= 2^{-1}(\chi_{N1} + \chi_{N2} + \chi_{N3} + \chi_{N4}) \\ \xi_4 &= 2^{-1}(\chi_{N1} + \chi_{N2} - \chi_{N3} - \chi_{N4}) \\ \xi_5 &= 2^{-1}(\chi_{N1} - \chi_{N2} - \chi_{N3} + \chi_{N4}) \\ \xi_6 &= 2^{-1}(\chi_{N1} - \chi_{N2} + \chi_{N3} - \chi_{N4})\end{aligned}$$

where χ_{Ca} and χ_{Cb} indicate the two $2p\pi$ -AO's on the C atoms of the C=C group and χ_{Ni} the lone-pair AO on the i -th N atom (Fig. 6(B)). The MO's of the whole molecule, ϕ , are, then, expressed as follows,

$$\phi = \sum c_i \xi_i$$

where c_i is a proper coefficient. The overlap integrals, S_{NN} and S_{CN} , are neglected, while S_{CC} is included and taken to be 0.257.

The two matrix elements, H_{11} and H_{22} ($H_{ii} = \int \xi_i H \xi_i d\tau$ where H indicates the effective one-electron Hamiltonian of the whole molecule), are assumed to be equal to -10.5 and -3.0 eV, respectively, empirically from the ionization potential and the excitation energy to the first excited singlet ($^1\Sigma_u^+$) state of ethylene. The four matrix elements, H_{33} , H_{44} , H_{55} , and H_{66} , are given as simple sums of the nitrogen Coulomb integral, α_N , and various resonance integrals between two nitrogen atoms, β_{NN} . α_N is taken to be -8.0 eV from the vertical ionization potential estimated for $N(C_2H_5)_3$. The β_{NN} 's are found to play an important role in the case of TMAE and included in the calculation, although they were neglected in the MO calculations made for TMAE previously.⁴ These integrals are calculated from the equations of the type, $\beta_{NN} = S_{NN}(\beta_{CC}/S_{CC})$, where S_{NN} is the overlap integral between two nitrogen atoms, and β_{CC} and S_{CC} are taken to be -3.8 eV and 0.257, respectively. The calculation of S_{NN} is made by the use of Mulliken's table.²⁰ The Slater's parameter ($\mu = Z_{eff}/n^*$) for a nitrogen $2p$ AO calculated by ordinary Slater's rule is 1.95. However, a little smaller value may be more suited for a μ value of a nitrogen lone-pair AO. In the present work, calculations were made using two μ values of 1.95 and 1.80. It turned out that there was almost no substantial difference between the results obtained for the two μ values. The off-diagonal matrix elements, H_{ij} ($i \neq j$), are expressed in terms of β_{CN} , the resonance integral between the adjacent C and N atoms, which is calculated from the equation, $\beta_{CN} = 0.8\beta_{CC}\sin\theta$, where β_{CC} is taken to be -2.5 eV by considering that the C-N distance is longer than the C=C distance of ethylene and θ is the twisting angle of the dialkylamino group defined before. The other parameters used are as follows; the bond distance, $R(C=C) = 1.34$ Å, $R(C-N) = 1.37$ Å and the bond angle, $\angle NCN = \angle NCC = 120^\circ$.

Transition moments are calculated by assuming $\int \chi_p r \chi_q d\tau = 0$ if $p \neq q$. The center of the charge density of the lone-pair AO is assumed to lie at 0.3 Å away from the nitrogen nucleus in the direction of the sp^3 hybrid orbital.

20) R. S. Mulliken, C. A. Rieke, D. Orloff, and H. Orloff, *J. Chem. Phys.*, **17**, 1248 (1949).